

# Temperature Dependence of the Chemical Potential in $\text{Na}_x\text{CoO}_2$ : Implications for the Large Thermoelectric Power

Yukiaki Ishida<sup>1</sup>, Hiromichi Ohta<sup>2,3</sup>, Atsushi Fujimori<sup>1</sup>, Hideo Hosono<sup>3,4</sup>

<sup>1</sup>*Department of Physics and Department of Complexity Science and Engineering,  
University of Tokyo, Kashiwa, Chiba 277-8561, Japan,*

<sup>2</sup>*Graduate School of Engineering, Nagoya University, Furo-cho, Chikusa, Nagoya 464-8603, Japan,*

<sup>3</sup>*ERATO-SORST, JST, in Frontier Collaborative Research Center,  
S2-6F East, Mail-box S2-13, Tokyo Institute of Technology,*

*4259 Nagatsuta-cho, Midori-ku, Yokohama 226-8503, Japan and*

<sup>4</sup>*Frontier Collaborative Research Center, S2-6F East, Mail-box S2-13,*

*Tokyo Institute of Technology, 4259 Nagatsuta-cho, Midori-ku, Yokohama 226-8503, Japan*

(Dated: October 18, 2018)

We have performed a temperature-dependent photoemission study of a  $\text{Na}_x\text{CoO}_2$  ( $x \sim 0.8$ ) epitaxial thin film prepared by the reactive solid-phase epitaxy method. The chemical potential shift as a function of temperature was derived from the Co 3d peak shift, and revealed a crossover from the degenerate Fermion state at low temperatures to the correlated hopping state of  $\text{Co}^{3+}/\text{Co}^{4+}$  mixed-valence at high temperatures. This suggests that the large thermoelectric power at high temperatures should be considered in the correlated hopping picture.

PACS numbers: 72.15.Jf, 71.28.+d, 79.60.-i

Thermoelectric (TE) materials directly convert heat into electricity. Extensive effort has been made on search for efficient TE materials for practical applications such as Peltier refrigerators and TE batteries [1, 2, 3]. While heavily doped semiconductors have been considered as promising TE materials, the recent report on the large TE power in  $\text{Na}_x\text{CoO}_2$  ( $x > 0.5$ ,  $\sim 100 \mu\text{V}/\text{K}$  at room temperature) attracted much interest because it also showed metallic and hence high conductivity [4]. In conventional metals, one expects small TE power caused by metallic diffusion typically of several  $\mu\text{V}/\text{K}$  arising from the energy dependence of the conductivity around the electron chemical potential  $\mu$  [1, 5]. Thermodynamic properties of metallic  $\text{Na}_x\text{CoO}_2$  ( $x > 0.5$ ) are also anomalous: it exhibits a large electronic specific-heat coefficient [6] and a Curie-Weiss magnetic susceptibility [7], which can be attributed to strong electron correlation [8]. Therefore, it should be clarified whether the origin of the large TE power involves strong electron correlation effects or not. Based on the strong correlation limit, Koshihase, Tsutsui and Maekawa [9] explained the large TE using a Heikes formula to include the spin-orbital degeneracy of the  $\text{Co}^{3+}$  and  $\text{Co}^{4+}$  ions. On the other hand, the largeness of the TE was discussed within the Boltzmann transport theory [10, 11].

By photoemission spectroscopy (PES), one measures the single-particle spectral function whose energy abscissa is referenced to  $\mu$ . Therefore, PES is a powerful tool not only to investigate the quasi-particle (QP) dynamics of materials but also the thermodynamic quantities like  $\mu$  [12, 13, 14]. Previous PES studies on bulk  $\text{Na}_x\text{CoO}_2$  ( $x > 0.5$ ) have revealed a QP peak developing in the narrow energy region within  $\sim 100$  meV from  $\mu$  [15, 16, 17]. The derived hopping amplitude  $t$  of the Co 3d electrons was extremely small ( $|t| \sim 10$  meV [16, 17]) compared to band-structure calculation ( $|t| \sim 130$  meV [10]), indicating

strong correlation effect. Interestingly, the QP peak disappeared above  $\sim 200$  K [15, 17], where the TE becomes large. Beyond the  $\sim 100$  meV region, the spectrum becomes broadened and dispersionless, and a Gaussian-like peak typical of low-spin  $t_{2g}$  electron systems is observed [16, 18]. This is in strong contrast to the band-structure calculations [10], where dispersions with typical bandwidths of  $\sim 1$  eV extend over the entire valence-band region. This discrepancy between band theory and PES spectra is reminiscent of the underdoped cuprates [19] and the colossal magnetoresistive manganites [20], where spectral weight near  $\mu$  is vanishingly small compared to strong incoherent structures residing at higher binding energies.

In this Letter, we report on the temperature dependence of the Co 3d-derived single-particle spectral function including the incoherent part to obtain the information about the position and temperature dependence of  $\mu$ , which would be non-trivial particularly above  $T \sim 200$  K where the QP disappears [15, 17]. Here, we have made temperature-dependent PES measurements on a single crystalline epitaxial thin film of  $\text{Na}_x\text{CoO}_2$  ( $x = 0.83$ ) [21]. Epitaxial thin film surfaces are, in general, stable compared to the fractured surfaces of bulk single crystals, and thus advantageous for surface sensitive PES measurements particularly for temperature cycling [22].

A  $\text{Na}_{0.83}\text{CoO}_2$  epitaxial thin film of the size  $\sim 5$  mm  $\times$  10 mm with film thickness  $\sim 150$  nm was prepared by the reactive solid-phase epitaxy (R-SPE) method. Details of the R-SPE method are described elsewhere [21]. After the final step of the R-SPE method, namely, after having annealed the sample with a yttria-stabilized-zirconia (YSZ) coverplate with  $\text{NaHCO}_3$  powder in an electric furnace, the sample was immediately transferred into the preparation chamber of the spectrometer. In order to recover the clean surface, the sample was again

covered with the YSZ plate and annealed under the 1 atmO<sub>2</sub> (99.9999 %) atmosphere for 30 min at 550°C using a Pt annealing system. After the surface treatment, the preparation chamber was quickly vented to  $\sim 1.0 \times 10^{-7}$  Torr, the YSZ plate was dropped off, and the sample was transferred without exposure to air into the main chamber (base pressure  $\sim 1 \times 10^{-10}$  Torr). The Al K $\alpha$  line ( $h\nu=1486.6$  eV) and the monochromatized He I line ( $h\nu=21.22$  eV) were used as excitation sources, and the photoelectrons were collected using a Scienta SES-100 analyzer. Typical energy resolution was 13 meV for He I and 0.8 eV for Al K $\alpha$ .

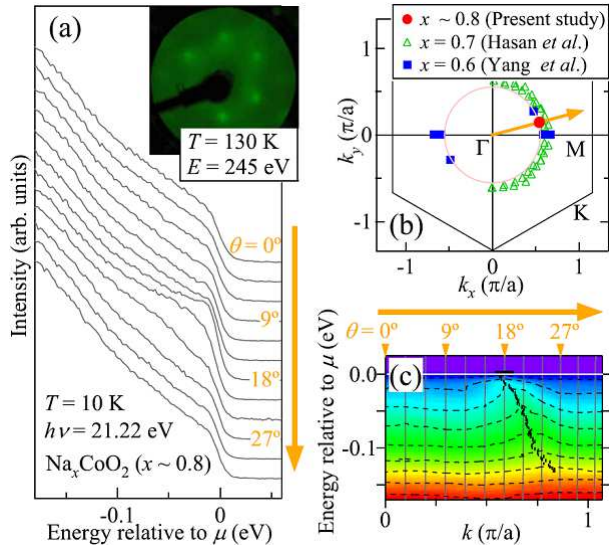


FIG. 1: (Color) ARPES spectra of Na<sub>x</sub>CoO<sub>2</sub> thin film prepared using the R-SPE method. (a) Energy distribution curves. Inset: LEED pattern for electron beam energy of 245 eV. (b) Brillouin zone of the triangular lattice. Orange arrow indicates the direction of the recorded dispersion.  $k_F$ 's determined from the present study and those reported by Yang *et al.* [16] and Hasan *et al.* [17] are indicated. (c) Intensity plot in the  $E$ - $k$  plane. Red/blue corresponds to high/low intensity. QP dispersion is traced by the black dots.

Figure 1(a) shows the angle-resolved PES (ARPES) spectra of the Na<sub>x</sub>CoO<sub>2</sub> thin film. We observed a clear dispersion from the  $\Gamma$  point toward the Brillouin zone boundary along a cut indicated by an orange arrow in Fig. 1(b), as well as the six-fold LEED pattern shown in the inset of Fig. 1(a) reflecting the triangular lattice. A virtually carbon-free surface was confirmed using core-level PES, while the O 1s spectra revealed a small contamination peak (5 % intensity of the O 1s main peak), which was presumably due to adsorbed oxygen after the *in situ* oxygen annealing. These results indicate that a clean single crystalline surface was obtained after the R-SPE treatment. The QP dispersion crosses  $\mu$  at  $k_F \sim 0.56 \frac{\pi}{a}$  ( $a$ : Co-Co distance) in the  $E$ - $k$  plane [Fig. 1(b)]. From comparison with the previous studies [16, 17], the present Fermi-surface volume is in the range of  $\sim 0.6 < x < \sim 0.8$  [Fig. 1(b)], in agreement with

the value  $x=0.83$  determined from the lattice constant [21]. This indicates that the Na evaporation during the oxygen annealing was successfully minimized even at the outermost layer of the thin film by using the YSZ coverplate, and we were probing the electronic structure in the Curie-Weiss metal phase ( $x > 0.5$ ) showing the large TE power [23]. Hereafter, we consider the Na concentration of the measured Na<sub>x</sub>CoO<sub>2</sub> surface to be  $x \sim 0.8$ .

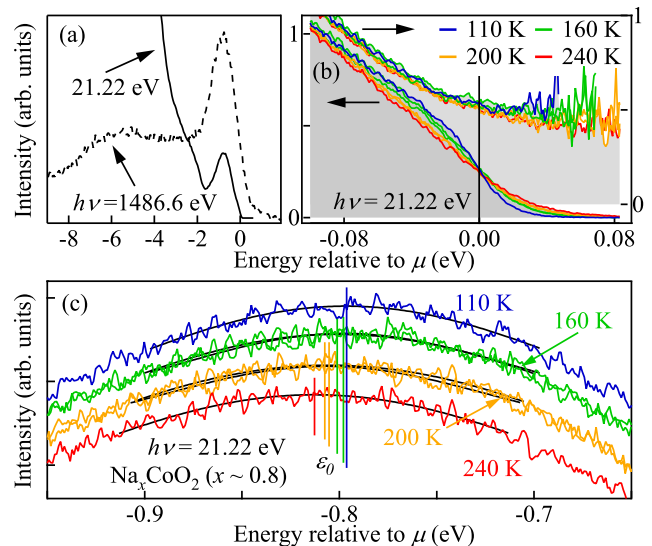


FIG. 2: (Color) Temperature dependence of the angle-integrated PES spectra of Na <sub>$\sim 0.8$</sub> CoO<sub>2</sub>. (a) Valence-band spectra using photon energies of 21.22 eV and 1486.6 eV. (b) Temperature dependence of PES spectra in the region near  $\mu$  (left axis). The temperature was cycled as 160 $\rightarrow$ 110 $\rightarrow$ 160 $\rightarrow$ 200 $\rightarrow$ 240 $\rightarrow$ 200 (in units of K). The spectra divided by the Fermi-Dirac function are also plotted (right axis). (c) Temperature dependence in the Co 3d  $t_{2g}$  peak region. Spectra have been offset according to the measuring temperature. The fitted Gaussian curves and the vertical bars indicating the peak positions are overlaid.

Next, we studied temperature dependence of the Co 3d-derived peak which is centered at  $\sim 0.8$  eV below  $\mu$  as shown in Fig. 2. Here we note that the  $\sim 0.8$  eV peak was observed even when we increased the bulk sensitivity of PES using the higher excitation energy of 1486.6 eV, as shown in Fig. 2(a). This suggests that the broad  $\sim 0.8$  eV peak and the smallness of the QP spectral weight near  $\mu$  are intrinsic bulk electronic properties. The spectra at various temperatures near  $\mu$  are plotted in Fig. 2(b) (left axis). We have also plotted the spectra divided by the Fermi-Dirac function so as to obtain the information about the DOS around  $\mu$ . At low temperatures, one can see a clear Fermi cut-off, reflecting the metallic character of Na<sub>x</sub>CoO<sub>2</sub> [4], and a negative slope in the DOS around  $\mu$ , which, within the degenerate-Fermion model, can cause an upward shift of  $\mu$  with temperature (described later). The spectra show that the temperature dependence near  $\mu$  is largely due to that of the Fermi-Dirac function. On the other hand, as shown in Fig.

2(c), the enlarged plot around 0.8 eV shows that the Co  $3d$   $t_{2g}$  peak is shifted to higher binding energies with temperature. A similar tendency was observed in the ARPES study of Ref. [17]. Although not so accurate, the temperature dependent shifts in core-level spectra (not shown) were also consistent with that of the Co  $3d$  peak. Since the temperature dependent shift of Co  $3d$  peak occurred reproducibly during the temperature cycling, one can attribute it to intrinsic changes of the electronic structure and not to the sample surface degradation during the temperature cycling. Here, the Co  $3d$   $t_{2g}$  peak positions ( $\varepsilon_0$ ) have been determined by fitting the region  $\sim -0.8 \pm 0.1$  eV to Gaussians, and are indicated by vertical bars. The deduced  $T$ -dependent peak shift was independent of the different fitted energy range.

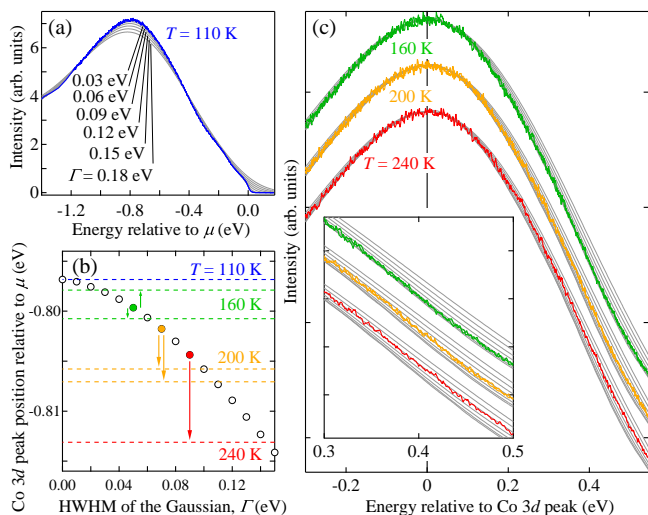


FIG. 3: (Color) Temperature broadening and shift of the Co  $3d$  peak. (a) A library of Gaussian broadened 110 K spectra. (b) Co  $3d$  peak position of the library spectra as a function of  $\Gamma$  (open circles) and the Co  $3d$  peak positions ( $\varepsilon_0$ ) (dashed lines). (c) Comparison of the line shapes of spectra with the library spectra. The library spectra for  $0 < \Gamma < 0.15$  eV with 0.02-eV intervals are shown with thin solid curves. All the spectra have been normalized to the Co  $3d$  peak height, and the energies have been referenced to the Co  $3d$  peak position. Inset shows an enlarged plot of the lower binding energy side of the peak.

We shall show below that the  $T$ -dependent Co  $3d$  peak shift can be explained by a combination of a broadening-induced shift of the asymmetric Co  $3d$  peak and an extra  $T$ -dependent shift. We attribute the latter shift to the chemical potential shift,  $\Delta\mu$  [24]. First, we show how the Co  $3d$  peak was broadened with temperatures. In Fig. 3(a), we have constructed a library of Gaussian-convoluted 110 K spectrum. Since the Co  $3d$  peak was asymmetric, the peak position of the convoluted spectrum was shifted to lower energies as the half width at half the maximum ( $\Gamma$ ) of the Gaussian was increased [see, Fig. 3(b)]. Then, as shown in Fig. 3(c), in order to reproduce the line shapes, we chose from the library the  $\Gamma$ 's for

the  $T=160, 200,$  and  $240$  K spectra as  $\Gamma=0.05, 0.07,$  and  $0.09$  eV, respectively. The Co  $3d$  peak position is shifted with such broadening since the Co  $3d$  peak position is asymmetric. However, this broadening-induced peak shift [indicated by filled circles in Fig. 3(b)] was not enough to explain the recorded peak shift, that is, there were extra  $T$ -dependent peak shifts as indicated by arrows in Fig. 3(b). We have interpreted this extra shift as  $\Delta\mu$ , and have plotted it in Fig. 4. We have also plotted the relative Co  $3d$  peak shifts recorded during the cooling series at  $T < 150$  K. In this temperature range, the  $T$ -dependent broadening of the Co  $3d$  peak was suppressed, and only the  $T$ -broadening of the Fermi-Dirac function near  $\mu$  was detectable.

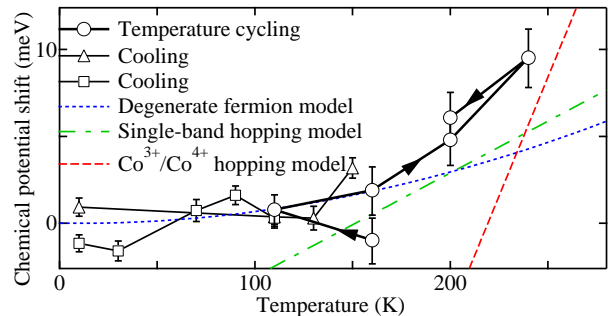


FIG. 4: (Color) Chemical potential shift  $\Delta\mu$  of  $\text{Na}_x\text{CoO}_2$  ( $x \sim 0.8$ ) derived from the PES spectra.  $\Delta\mu$  estimated from the degenerate Fermion model and the slopes of  $\Delta\mu$ 's for the single-band hopping [25] and correlated-hopping model of low-spin  $\text{Co}^{3+}/\text{Co}^{4+}$  mixed-valence state [9] are plotted for comparison (see, text).

In conventional metals in which charge carriers are degenerate Fermions, finite  $\frac{\partial\mu}{\partial T}$  arises from the finite slope in the DOS around  $\mu$ .  $\Delta\mu$  is estimated within this model using the DOS in the inset of Fig. 2(a) and plotted in Fig. 4 (dotted line). One notice that the experimentally derived  $\Delta\mu$  deviates from the degenerate Fermion model above  $\sim 200$  K. This temperature coincides with the temperature above which the QP peak disappears in the ARPES spectra [15, 17]. The results may be interpreted as follows: Above the characteristic temperature  $T^* \sim 200$  K, the broadening of the Fermi-Dirac function  $\sim 4k_B T$  exceeds the width of the narrow QP band  $\sim 100$  meV [16, 17]. Then, the QP's can no more be described as degenerate Fermions and behave as classical particles undergoing thermally activated correlated hopping among the Co sites. For such carriers, the configuration entropy density  $s$  and hence  $\frac{\partial\mu}{\partial T} = -\frac{\partial s}{\partial x}$ , where  $x$  is the number of electron carriers per site, can be calculated following Ref. [25]. In the case of  $\text{Co}^{3+}/\text{Co}^{4+}$  mixed-valence state [9],

$$\frac{\partial\mu}{\partial T} = -k_B \ln\left(\frac{g_3}{g_4} \frac{1-x}{x}\right), \quad (1)$$

where  $g_3$  and  $g_4$  are the spin-orbital degeneracies of  $\text{Co}^{3+}$  and  $\text{Co}^{4+}$ , respectively, and  $x$  is the fraction of

Co<sup>3+</sup> ions. Here, we note that the presence of electron-boson coupling does not affect Eq. (1). In Fig. 4, we have plotted  $\Delta\mu = -k_B \ln\left(\frac{g_3}{g_4} \frac{1-x}{x}\right) \times T + \text{const.}$  for  $g_3=1, g_4=6$ , and  $x=0.8$ , corresponding to the low-spin Co<sup>3+</sup>/Co<sup>4+</sup> mixed-valence state with a dashed line [9], and that for  $g_3=1, g_4=2$ , and  $x=0.8$  with a dot-dashed line, which corresponds to the single-band hopping model [25]. One can recognize that the experimentally derived  $\Delta\mu$  crossovers at  $T^*$  from the degenerate Fermion model to the localized-electron model as the temperature is increased.

The above result for  $\Delta\mu$  suggests that the transport properties should also be treated within the correlated hopping model in the high temperature regime  $T>T^*$  [25]. First of all, the largeness of the TE power has indeed been attributed to the large spin-orbital entropy of low-spin Co<sup>3+</sup>/Co<sup>4+</sup> mixed-valence state, since, at high enough temperatures, the TE power (Seebeck coefficient) is dominated by the entropy term  $\frac{\mu}{T}$  compared to the energy-transport term associated with the kinetic energies of carriers [9, 25, 26]. The high temperature Hall coefficient also shows anomalous increase with  $T$  [23, 27], and its origin was discussed in terms of the hopping effect on the triangular lattice of Co<sup>3+</sup>/Co<sup>4+</sup> [27, 28]. On the other hand, the suppressed  $\Delta\mu$  at the low temperature regime  $T<T^*$  indicate that the carriers are degenerate, and hence Boltzmann type transport for degenerate Fermion model may become valid [10, 11]. Nevertheless, the novel magnetic-field suppression of the TE

power is observed already at  $T=2.5$  K [29]. DC resistivity indicates anomalously large electron-electron scattering rate at  $T<1$  K, which is also suppressed in a magnetic field [30]. These observations indicate that the degenerate Fermion excitations below  $T^*$  has another low energy/temperature scale ( $\ll 200$  K) influenced by strong correlation.

In conclusion, the experimentally derived chemical potential shift as a function of temperature in Na<sub>x</sub>CoO<sub>2</sub> revealed a crossover from the low-temperature degenerate Fermion state to the high-temperature correlated hopping state involving the spin-orbital degeneracy of the Co<sup>3+</sup>/Co<sup>4+</sup> mixed-valence at a characteristic temperature  $T^*\sim 200$  K. The anomalous transport properties at high temperatures such as the large TE power and the unsaturated Hall coefficient with temperatures should thus be treated within the correlated hopping model. The present work has demonstrated that the temperature-dependent chemical potential shift can be used as a measure of correlation effects in orbitally degenerate systems.

We thank K. Sugiura for collaboration, T. Mizokawa, K.M. Shen and K. Okazaki for discussion, K. Tanaka, H. Yagi, H. Wadati, M. Hashimoto, M. Takizawa and M. Kobayashi for help in experiment. This work was supported by a Grant-in-Aid for Scientific Research in Priority Area (16204024) from the Ministry of Education, Culture, Sports, Science and Technology, Japan.

- 
- [1] G. Mahan, B. Sales, and J. Sharp, *Phys. Today* **50** No. 3, 42 (1997).
- [2] F.J. DiSalvo, *Science* **285**, 703 (1999).
- [3] B.C. Sales, *Science* **295** 1248 (2002).
- [4] I. Terasaki, Y. Sasago, and K. Uchinokura, *Phys. Rev. B* **56**, R12685 (1997).
- [5] R.D. Barnard, *Thermoelectricity in metals and alloys* (Taylor & Francis, London, 1972).
- [6] Y. Ando, N. Miyamoto, K. Segawa, T. Kawata, and I. Terasaki, *Phys. Rev. B* **60**, 10580 (1999).
- [7] R. Ray, A. Ghoshray, K. Ghoshray, and S. Nakamura, *Phys. Rev. B* **59**, 9454 (1999).
- [8] M. Imada, A. Fujimori, and Y. Tokura, *Rev. Mod. Phys.* **70**, 1039 (1998).
- [9] W. Koshibae, K. Tsutsui, and S. Maekawa, *Phys. Rev. B* **62**, 6869 (2000).
- [10] D.J. Singh, *Phys. Rev. B* **61**, 13397 (2000).
- [11] T. Takeuchi, T. Kondo, T. Takami, H. Takahashi, H. Ikuta, U. Mizutani, K. Soda, R. Funahashi, M. Shikano, M. Mikami, S. Tsuda, T. Yokoya, S. Shin, and T. Muro, *Phys. Rev. B* **69**, 125410 (2004).
- [12] A. Ino, T. Mizokawa, A. Fujimori, K. Tamasaku, H. Eisaki, S. Uchida, T. Kimura, T. Sasagawa, and K. Kishio, *Phys. Rev. Lett.* **79**, 2101 (1997).
- [13] A. Fujimori, A. Ino, J. Matsuno, T. Yoshida, K. Tanaka, and T. Mizowaka, *J. Electron Spectrosc. Relat. Phenom.* **124**, 127 (2002).
- [14] K.M. Shen, F. Ronning, D.H. Lu, W.S. Lee, N.J.C. Ingle, W. Meevasana, F. Baumberger, A. Damascelli, N.P. Armitage, L.L. Miller, Y. Kohsaka, M. Azuma, M. Takano, H. Takagi, and Z.-X. Shen, *Phys. Rev. Lett.* **93**, 267002 (2004).
- [15] T. Valla, P.D. Johnson, Z. Yusof, B. Wells, Q. Li, S.M. Loureiro, R.J. Cava, M. Mikami, Y. Mori, M. Yoshimura, and T. Sasaki, *Nature (London)* **417**, 627 (2002).
- [16] H.-B. Yang, S.-C. Wang, A.K.P. Sekharan, H. Matsui, S. Souma, T. Sato, T. Takahashi, T. Takeuchi, J.C. Campuzano, R. Jin, B.C. Sales, D. Mandrus, Z. Wang, and H. Ding, *Phys. Rev. Lett.* **92**, 246403 (2004).
- [17] M.Z. Hasan, Y.-D. Chuang, D. Qian, Y.W. Li, Y. Kong, A.P. Kuprin, A.V. Fedorov, R. Kimmerling, E. Rotenberg, K. Rosnagel, Z. Hussain, H. Koh, N.S. Rogado, M.L. Foo, and R.J. Cava, *Phys. Rev. Lett.* **92**, 246402 (2004).
- [18] T. Mizokawa, L.H. Tjeng, P.G. Steeneken, N.B. Brookes, I. Tsukada, T. Yamamoto, and K. Uchinokura, *Phys. Rev. B* **64**, 115104 (2001).
- [19] A. Damascelli, Z. Hussain, and Z.-X. Shen, *Rev. Mod. Phys.* **75**, 473 (2003).
- [20] D.S. Dessau, T. Saitoh, C.-H. Park, Z.-X. Shen, P. Villella, N. Hamada, Y. Moritomo, and Y. Tokura, *Phys. Rev. Lett.* **81**, 192 (1998).
- [21] H. Ohta, S.-W. Kim, S. Ohta, K. Koumoto, M. Hirano, and H. Hosono, *Cryst. Growth Des.* **5**, 25 (2005).
- [22] K. Okazaki, A. Fujimori, T. Yamauchi, and Y. Ueda,

- Phys. Rev. B **69**, 140506(R) (2004).
- [23] M.L. Foo, Y. Wang, S. Watauchi, H.W. Zandbergen, T. He, R.J. Cava, and N.P. Ong, Phys. Rev. Lett. **92**, 247001 (2004).
- [24] Since the  $t_{2g}$  orbital is nearly filled, the Co  $3d$  peak can be approximately regarded as a shallow core level being a good measure of  $\mu$ .
- [25] P.M. Chaikin and G. Beni, Phys. Rev. B **13**, 647 (1976).
- [26] W. Koshibae and S. Maekawa, Phys. Rev. Lett. **87**, 236603 (2001).
- [27] Y. Wang, N.S. Rogado, R.J. Cava, and N.P. Ong, cond-mat/035455.
- [28] B. Kumar and B.S. Shastry, Phys. Rev. B **68**, 104508 (2003).
- [29] Y. Wang, N.S. Rogado, R.J. Cava, and N.P. Ong, Nature (London) **423**, 425 (2003).
- [30] S.Y. Li, L. Taillefer, D.G. Hawthorn, M.A. Tanatar, J. Paglione, M. Sutherland, R.W. Hill, C.H. Wang, and X.H. Chen, Phys. Rev. Lett. **93**, 056401 (2004).